



Raman signal enhancement of low-cost metal sheet SERS with gold decoration

Nampueng PANGPAIBOON¹, Kawinphob PHETNAM¹, Sukon KALASUNG², Chanunthorn CHANANONAWATHORN², Viyapol PATTHANASETTAKUL², Mati HORPRATHUM², Pitak EIAMCHAI², Noppadon NUNTAWONG², and Saksorn LIMWICHEAN^{2,*}

¹Department of Industrial Physics and Medical Instrumentation, Faculty of Applied Science, King Mongkut's University of Technology North Bangkok, Bangkok, 10800, Thailand

²Opto-Electrochemical Sensing Research Team, Spectroscopic and Sensing Devices Research Group, National Electronics and Computer Technology Center, Pathum Thani, 12120, Thailand

*Corresponding author e-mail: saksorn.limwicheckan@nectec.or.th

Received date:

12 May 2021

Revised date:

15 September 2021

Accepted date:

15 October 2021

Keywords:

Laser-engraved;
Sputtering;
Zinc SERS;
Copper SERS;
Low-cost SERS

Abstract

Surface Enhance Raman Spectroscopy (SERS) is a sensitive surface creating plasmonic resonance for the Raman scattering. SERS is considered as a powerful technique to enhance the Raman signal, when quantity of sample is limited. Recently, our lab team has discovered a low-cost SERS template fabrication, laser-engraving method, which is suitable with gold nanoparticles decoration. In this work, two different materials, zinc, and copper, were used as metal sheet SERS substrate. Gold nanoparticles sputtered with 270 s of sputtering time were used as decorated noble metal. FE-SEM images illustrated the nano-in-microstructure of the engraved metal sheets. The decorated Au nanoparticles were uniform and fully cover on the rough metal sheet templates. From contact angle measurement with DI water, Zn/Au SERS provided the highest contact angle, which was 142.10 ± 0.51 degree. SERS performance, including Enhancement Factor (EF), Limit of Detection (LOD), and shelf-life were investigated. The EF values of Zn/Au SERS and Cu/Au SERS were 7.40×10^9 and 1.70×10^8 , respectively. From LOD results, Zn/Au SERS presented the great ability to enhance the Raman signal at 10^{-7} molar concentration. However, after 90 days of shelf-life test, both showed the capability to enhance the Raman signal.

1. Introduction

Surface Enhance Raman Spectroscopy (SERS) is one of the influential analytic innovations. Raman spectroscopy provides a characteristic fingerprint which can identify a molecule of substance. Nowadays, SERS is used as an ultra-sensitive surface for detecting chemical and biological species in many applications; for example, detecting herbicide in agriculture [1-3], and detecting addictive or explosive substance in forensic science [4-6]. The significant advantages of SERS, non-destructiveness, and fast sensing, make SERS become an interesting appliance for Raman spectroscopy. In principle, SERS can enhance the Raman signal by surface plasmon resonance (SPR). This phenomenon occurs at the surface of noble metal when free-electrons cloud is vibrated by monochromatic light excitation. There are three types of SERS, including colloid base [7,8], thin-film base [9,10], and 3D-hybrid structure [3,11-15]. The conventional colloid base is not satisfied as a strong enhancement of Raman signal. This structure requires complex and high-cost process and produces non-repeatability device. For thin-film base structure, even it presents an ability to enhance the Raman signal strongly; however, thin film structure requires complex and high-cost process as same as the colloid base. Afterwards, 3D-hybrid structure is developed for reducing cost and simplify fabrication

process. This structure is constructed with a nano-in-microstructure template decorated by the noble metal nanoparticles.

There are many methods to fabricate the 3D-hybrid structure SERS; for example, lithography [16-19], physical vapor deposition (PVD) [3,20-24], chemical vapor deposition (CVD) [25-27], hydrothermal [28-30] and laser marking [3,31-33]. From all these methods, laser marking or, laser engraving is an interesting one because of low-cost production, easy processing, and non-chemical waste technique. Recently, our research team has successfully fabricated SERS from an aluminum sheet by using laser engraving technique. We found that the laser-engraved aluminum sheet SERS decorated with Au nanoparticles presented high intensity and high stability Raman signal [3]. From the success, we are interested to discover a set of low-cost SERS template made by inexpensive material and present high efficiency as SERS device.

Considering the intended application and economic, zinc (Zn) has received much attention in industries due to its non-toxic and high electric performance. Additionally, zinc is the fourth most common metal use in production, just below of iron, aluminum, and copper [34]. For SERS application, zinc sheet has been reported to use as SERS substrate; for example, a novel and reproducible Zn/Au-Ag/Ag sandwich-structure SERS substrate discovered by Wang *et al.*

in 2021 [35]. With the composite substrate, SERS demonstrated high sensitivity with a wide dynamic range because of a rough structure and its interfacial charge transfer. On the other hand, copper (Cu) substrate was proof that it is a good choice of SERS template because of highly efficient SERS platform with a low detection limit, good recyclability, and a long service time under ambient conditions [32]. In addition, copper has good biocompatibility, high conductivity, and chemical stability, which supports a great potential in ultra-trace detection of biomolecules.

Therefore, in this paper, two commercial low-cost metal sheets, zinc and copper, have been selected as a laser-engraved template for Au nanoparticles. The Raman signal enhancement of two low-cost metal sheet SERS were investigated. Roughness surfaces of these metal sheets were created by using a conventional laser-marking machine which is simple and inexpensive. Sputtering technique was used to decorate Au nanoparticles, SPR material, on the SERS templates. Topography of the SERS surface, topography of the decorating nanoparticles, hydrophobic property of the SERS and ability of the Raman signal enhancement were investigated. Moreover, efficiency of SERS was verified by limit of detection (LOD test), enhancement factor (EF), and shelf-life. A good performance SERS produced by low-cost metal sheets and inexpensive techniques was expected for this research.

2. Experimental

2.1 Low-cost metal sheet SERS fabrication

Commercial zinc and copper sheets were selected to be an enhancing surface for the Raman signal. Two simple steps of metal sheet SERS fabrication are laser engraving, and noble metal decorating, as described by following. First, the clean zinc and copper sheet were engraved by a laser marking machine with wavelength 1064 nm (Smart mark, Photonics Science Co., Ltd). Laser power, fill spacing, and frequency used for laser engraving were 12 W, 0.02 mm, and 30 kHz, respectively. After that, the engraved zinc and copper sheets were coated with Au nanoparticles by magnetron sputtering system (lab-assembled, single-cathode PVD system). Base pressure for an ultra-high vacuum (UHV) sputtering system was 5×10^{-6} mbar. Au nano-particles deposition was performed at 3.0×10^{-3} mbar operating pressure for 270 s sputtering time. Cathode current and DC power for operating were 0.1 A and 90 W, respectively. Finally, all samples were cut into a square piece of 5×5 mm² dimension, attached on a glass slide, and sealed in metalized package. Then Au zinc sheet SERS (Zn/Au SERS) and Au copper sheet SERS (Cu/Au SERS)

were completely fabricated. The fabrication procedure of low-cost metal sheet SERS is shown in Figure 1.

2.2 Characterization

Topography of bare zinc and copper sheet were examined through a field-emission scanning electron microscopy (FE-SEM). As same as metal sheet, FE-SEM was also used to characterize structure of Au nanoparticles on the metal sheets template. Diameter of the nanoparticles were measured by image J software. Hydrophobic property on the SERS substrate was analyzed by dropping deionized water (DI water), about 20 μ L, on the center of SERS and measuring contact angles of DI water by contact angle machine. To verify an enhancement ability of Zn/Au SERS and Cu/Au SERS, Rhodamine 6G (R6G) with 1×10^{-5} molar concentration was used as a testing solution. Two milliliters of R6G were dropped on the SERS and left at room temperature for 30 min. After that, the Raman enhancements from Zn/Au SERS and Cu/Au SERS were examined by inVia Raman microscope from Renishaw. Laser wavelength, exposure time and magnification of Raman spectroscopy for the examination were 785 nm, 30 s and 5X, respectively. An ability to enhance the Raman signal at a very low concentration was also studied in this work by using limit of detection (LOD) test with R6G substance from 1×10^{-4} to 1×10^{-7} molar concentration. Enhancement factor (EF) for the Raman signal of Zn/Au SERS and Cu/Au SERS were calculated. Finally, shelf-life test was observed by keeping the SERS in an ambient environment for 90 days. The Raman signals were measured along the period.

3. Results and discussion

Zinc and copper sheet templates were completely fabricated by the laser marking method. Nano-in-microstructure of engraved zinc and copper sheets were investigated by FE-SEM, as shown in Figure 2(a)-(d). Figure 2(a) and (c) shows microstructure surface of bare zinc and copper sheets at 1 k magnification, and after engraving by laser marking, bare zinc sheet presents nano-in-microstructure at 100 k magnification, as shown in Figure 2(b). FE-SEM image illustrates a homogeneous rough surface and uniform pattern nano-in-microstructure of engraved zinc sheet. In the same way, after laser-engraved, the copper sheet surface is homogeneous. Through FE-SEM image exhibits non-uniform structure of engraved copper sheet, the nano-in-microstructure is obviously presented in Figure 2(d). From the result, the engraved metal sheets, both Zn and Cu, are suitable for using as a supporting template for SERS.

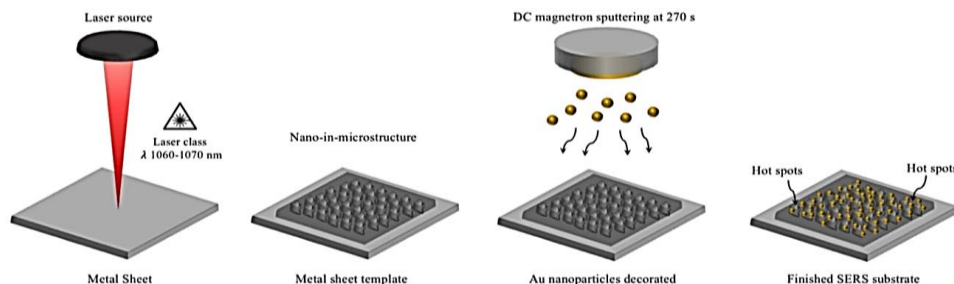


Figure 1. Schematic fabrication procedure for low-cost metal sheet substrate.

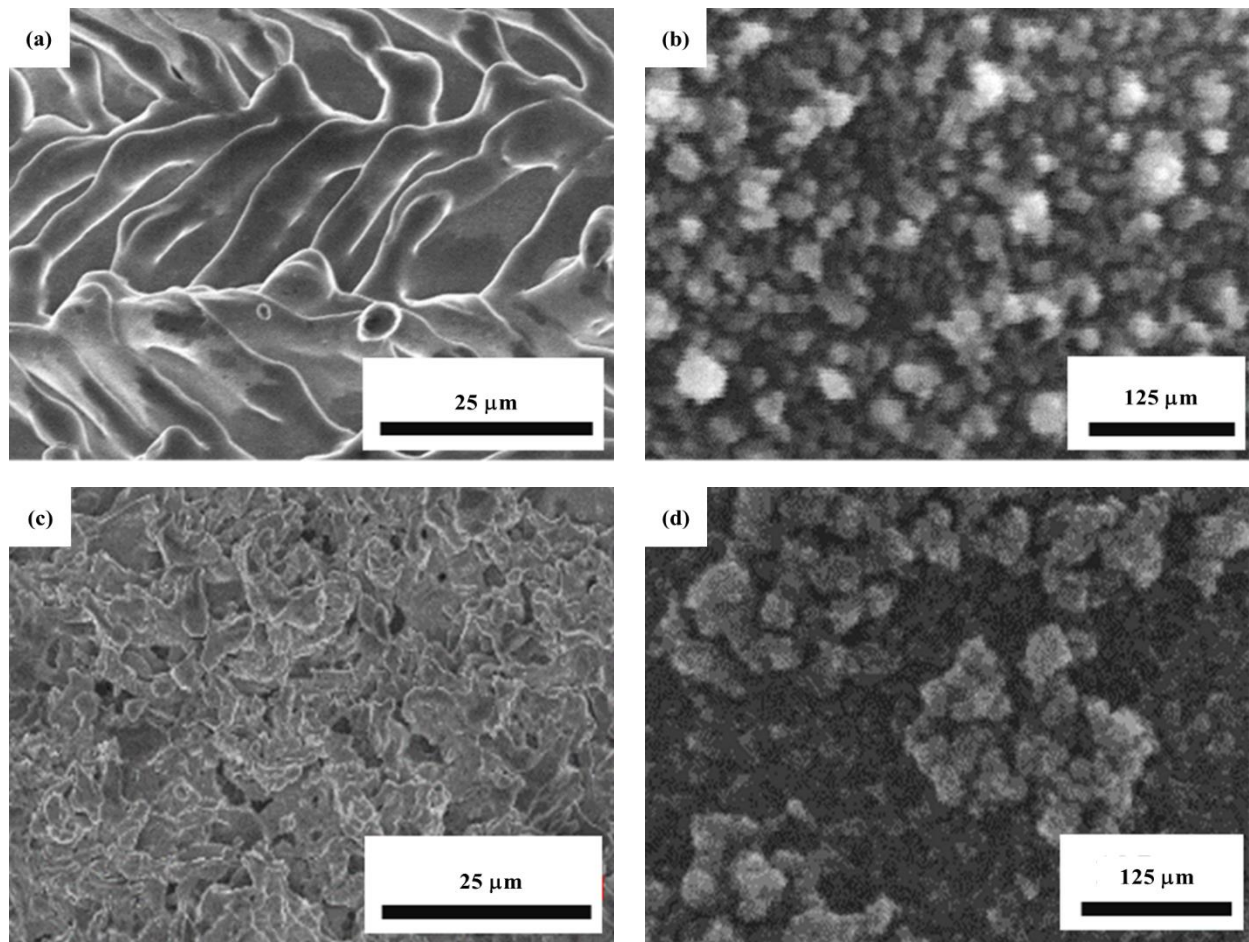


Figure 2. FE-SEM images illustrating by topography of bare zinc sheet and copper sheet (a) Bare zinc sheet after engraving at 1 k, (b) Bare zinc sheet after engraving at 100 k, (c) Bare copper sheet after engraving at 1 k, and (d) Bare copper sheet after engraving at 100 k.

After laser-engraved process, zinc and copper sheet templates were decorated with Au nanoparticle and then Zn/Au SERS and Cu/Au SERS were fabricated. Likewise, surface roughness of the engraved-metal sheets decorating with Au nanoparticles were investigated by FE-SEM. Topography images of Au nanoparticles on zinc and copper sheet templates are presented in Figure 3(a) and Figure 3(b), respectively. From FE-SEM, Au nanoparticles are spherical shape and formed as a cluster on the rough templates. The metal surfaces are fully covered

by a uniform distribution of Au nanoparticles. Average diameters of Au nanoparticles on zinc and copper sheet template are 44.87 ± 4.64 nm and 55.28 ± 6.03 nm, respectively. Because of the nanoparticle's aggregation, as shown in FE-SEM images, hot-spot or inter gap between the nanoparticles which is commonly used to identify the performance of SERS cannot be measured. Therefore, to predict enhancing ability of Zn/Au SERS and Cu/Au SERS, some characterization techniques were demonstrated in this part.

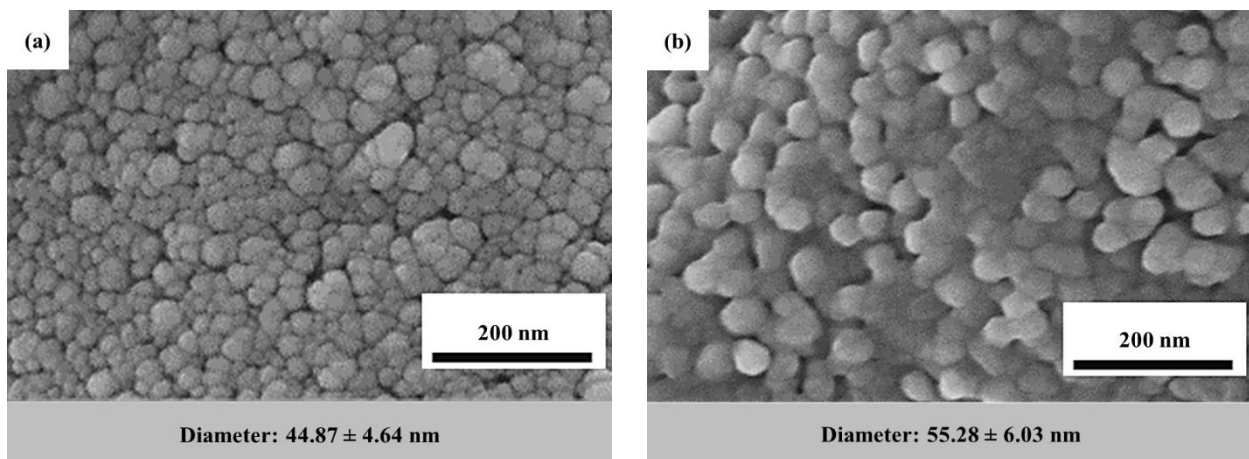


Figure 3. FE-SEM images illustrating by topography of Au nanoparticles decorated on (a) zinc sheet template, and (b) copper sheet template.

From literature reviews, hydrophobic property of SERS substrate can estimate an efficiency to enhance the Raman signal of SERS [12]. We found that contact angles of Zn/Au SERS and Cu/Au SERS are 142.1 ± 0.51 degree and 131.3 ± 0.41 degree, respectively, as shown in Figure 4(a)-(b). The higher contact angle of Zn/Au SERS, comparing with Cu/Au SERS, refers to probability of a strong Raman signal enhancement. Since small contact area between solution droplet and SERS substrate presents high concentration of a sample solution. After solution dry, molecule of the solution will settle at the bottom, in the small contact area. Therefore, this area will fully condense with molecule of solution, which increases an intensity of the Raman signal.

The Raman spectra of R6G testing solution on Zn/Au SERS and Cu/Au SERS are shown in Figure 5. Both of Zn/Au SERS and Cu/Au SERS can identify the characteristic Raman signal fingerprint of R6G molecule with the Raman shift at 610 cm^{-1} , 1367 cm^{-1} , and 1512 cm^{-1} . From Raman spectroscopy analysis, the Zn/Au SERS reveals higher intensity of the Raman signal than the Cu/Au SERS according to the results of hydrophobic test from the previous section. Comparing the Raman signal enhancement of our SERS with the commercial SERS chip (Onspec Nectec LITE SERS chip, Al/Au SERS), we found that the Zn/Au SERS shows the highest Raman intensity, following by the Al/Au Onspec SERS chip and the Cu/Au SERS, respectively.

For application, one of the important properties of SERS is an ability to enhance the Raman signal at a very low concentration solution. Therefore, the lowest concentration of testing solution that SERS can enhance the Raman signal were studied, which is called limit of detection (LOD) testing. LOD of Zn/Au SERS and Cu/Au SERS are tested by using 1×10^{-4} molar to 1×10^{-8} molar concentration of R6G solution. Figure 6(a) and (b) present LOD results of R6G Raman spectrum from Zn/Au SERS and Cu/Au SERS. The Raman shift of R6G Raman spectrum can be observed by the Zn/Au SERS until 1×10^{-7} molar concentration. After that, at 1×10^{-8} molar concentration, the Zn/Au SERS cannot provide the R6G Raman shift. On the other hand, the Cu/Au SERS can provide the R6G Raman shift until 1×10^{-6} molar concentration.

To investigate an enhancing efficiency of our SERS, enhancement factor (EF value) was calculated. EF value is widely used to report SERS performance [36]. This value represents an ability of SERS to enhance the Raman signal at any concentration of solution. EF value can be calculated by Equation (1).

$$EF = \left(\frac{I_{\text{surf}}}{I_{\text{bulk}}} \right) \times \left(\frac{N_{\text{bulk}}}{N_{\text{surf}}} \right) \quad (1)$$

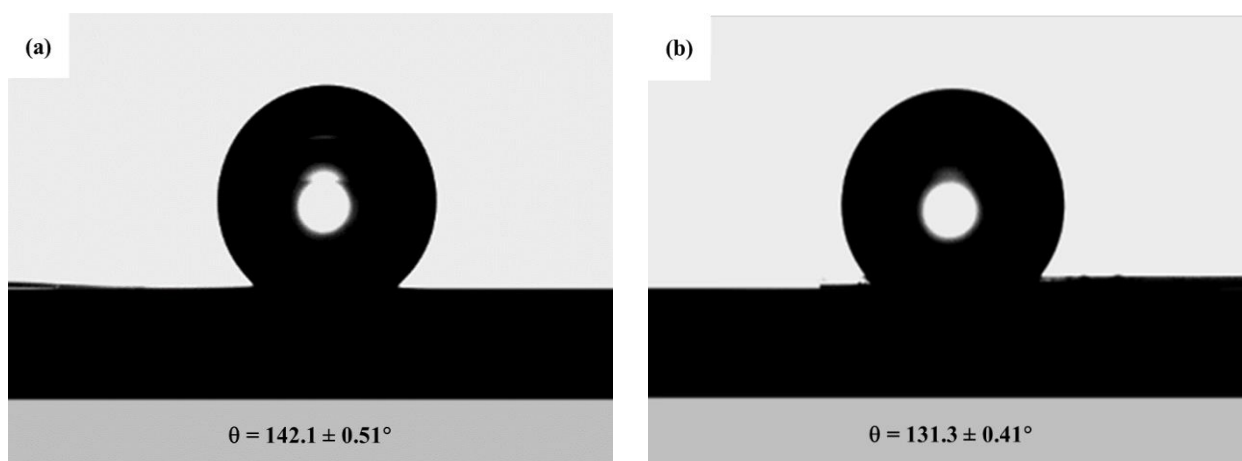


Figure 4. Contact angles of DI water droplet on (a) Zn/Au SERS, and (b) Cu/Au SERS.

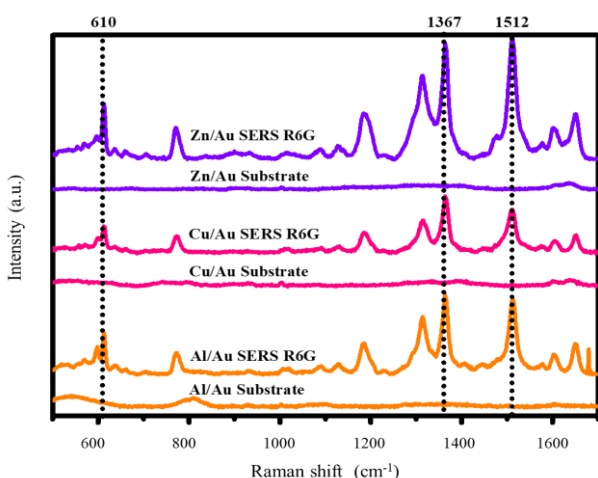


Figure 5. Raman spectra of R6G solution enhanced by Al/Au SERS, Cu/Au SERS and Zn/Au SERS.

As in the equation, I_{surf} is an intensity of the vibration modes on the SERS. I_{bulk} is the intensity of vibration mode from the Raman spectrum. N_{bulk} is the number of a molecules on the Raman spectrum. N_{surf} is the number of a probed molecules that upon the SERS surface. For this research, EF values of Zn/Au SERS, Cu/Au SERS, and the commercial Al/Au SERS (Onspec SERS chip) were calculated by using the Raman shift of R6G Raman spectrum at 1367 cm^{-1} as a reference peak. The EF values of Zn/Au and Cu/Au SERS are 7.40×10^9 and 1.70×10^8 , respectively. Zn/Au SERS shows higher EF value than Cu/Au SERS as expected. Moreover, comparing with the commercial Al/Au SERS, the EF value of our low-cost Zn/Au SERS is noticeably greater than of the commercial SERS, which is 4.13×10^9 . Besides, from literatures, EF values have been reported in the range of 5.49×10^6 to 4.20×10^7 [36-39]. Therefore, the low-cost metal sheet substrate, Zn/Au SERS and Cu/Au SERS present the impressive ability to enhance the Raman signal.

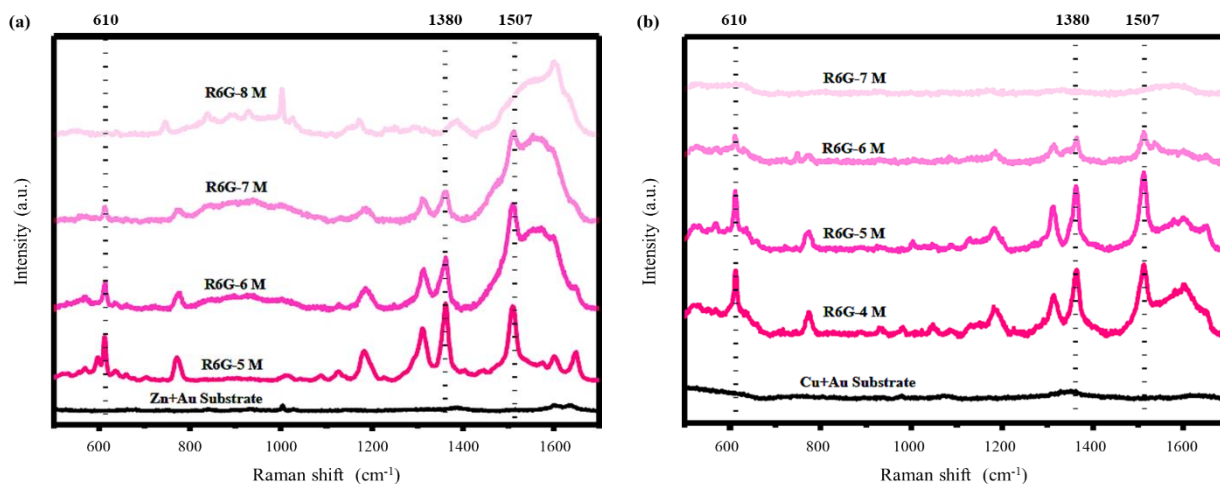


Figure 6. Limit of detection (LOD) of R6G solution from a) Zn/Au SERS and b) Cu/Au SERS.

The last examination, shelf-life test reveals an ability to enhance the Raman signal of SERS while keeping in an ambient environment for a long time. The intensities of the Raman signal were measured frequently along that period. SERS capability can be de-graded by three major factors: humidity, temperature, and pressure. In this experiment, shelf-life test of Zn/Au SERS and Cu/Au SERS were observed and compared with the commercial Al/Au Onspec SERS chip. R6G solution at 1×10^{-5} molar concentration was used as a testing solution. Data of the enhanced Raman signal intensities were collected for 90 days, and the results are presented in Figure 7. The intensities of R6G Raman spectrum relating with shelf-life (days) were calculated by using the average intensities of the reference peaks at 610 cm⁻¹, 1367 cm⁻¹, and 1512 cm⁻¹ of R6G Raman spectrum. Before shelf-life testing, the Zn/Au SERS presents the highest enhanced intensity of the Raman spectrum, following by the commercial Al/Au SERS and the Cu/Au SERS, and this trend remains for the first 7 days. During 14 days to 30 days, the Raman intensity from the Zn/Au SERS obviously decreases while the Raman intensity of the Cu/Au SERS turns to be the highest order. The Cu/Au SERS still presents higher Raman signal intensity than the Zn/Au SERS and the commercial Al/Au SERS for 90 days of our test. From the results, we found that both Zn/Au SERS and Cu/Au SERS have considerably efficiency to enhance the Raman signal. The Zn/Au SERS has a significant ability to enhance the Raman signal while the Cu/Au SERS presents a valuable long shelf-life advantage.

In practical using, SERS may be destroyed by many factors making SERS degradation, in this experiment, we try to observe the effects in the same way as normal use. Therefore, shelf-life properties were tested in an ambient environment. However, for suggestion, to increasing service life of SERS, the SERS should be stored in nitrogen-filled metalized bags as well as be controlled humidity and temperature during utilizing process.

From this research, we successfully fabricated low-cost metal substrate SERS, zinc and copper sheet, by using the simple and inexpensive laser engraving technique, which can reduce cost of production and improve the performance of SERS. The engraved zinc and copper sheets were sputtered with Au nanoparticles creating the surface plasmon resonance. The electron clouds from Au located on

the low-cost metal sheet perfectly amplify the Raman signal. We found that Zn/Au SERS and Cu/Au SERS reveal a good ability to enhance the Raman signal comparing with the literatures and the commercial one. From LOD testing and EF value, the Zn/Au SERS presents the highest efficiency as expected. It can enhance the Raman signal even when the concentration less to 1×10^{-7} molar concentration for R6G. The great performance of the Zn/Au SERS is a result of the homogeneous and uniform roughness surface. Moreover, the decorating Au nanoparticles are well-constructed with the engraved zinc nano-in-microstructure. This result harmonizes with the hydrophobic properties of the Zn/Au SERS which presented the high contact angle of DI water.

On the other hand, the Cu/Au SERS exhibits the remarkable result. Capability to enhance the Raman signal of the Cu/Au SERS remained constant until 90 days, which suitable for in general application. Since copper is a noble metal as same as Au, the electron clouds on the copper surface can cooperate with the electron clouds of Au nanoparticles. Then two materials mutually amplify the SPR mechanism which causes the performance of the Raman enhancement.

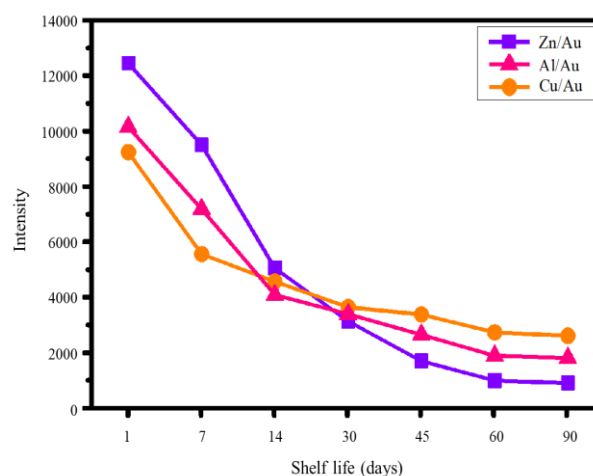


Figure 7. Relationship between shelf-life (days) and intensity of R6G Raman spectrum of Zn/Au SERS, Al/Au SERS, and a commercial SERS chip (Onspec Nectec LITE SERS chips, Al/Au SERS).

4. Conclusions

Low-cost metal SERS chips, Zn/Au SERS and Cu/Au SERS were successfully fabricated by laser-engraved technique. Topography images studied by FE-SEM reveal nano-in-microstructure of the engraved templates and the fully covered Au nanoparticles on these metal sheet surfaces. Hydrophobic property of the SERS surface can predict an ability to enhance the Raman signal. Performance of Zn/Au SERS and Cu/Au SERS were studied by measuring enhancement Raman intensity, calculating EF values, testing LOD and observing shelf-life. The Zn/Au SERS presents the high value of EF and better LOD results. Although the Cu/Au SERS shows longer period usability, both SERS are suit for general application and their performances are greater than the commercial SERS chip.

Acknowledgements

For our success in this research, we would like to thank National Electronics and Computer Technology Center (NECTEC), National Science and Technology Development Agency. This research was funded by King Mongkut's University of Technology North Bangkok, Thailand (KMUTNB-65-BASIC-19).

References

- [1] C. Chakaja, S. Limwichean, N. Nuntawong, P. Eiamchai, S. Kalasung, O.-U Nimitrakoolchai, and N. Hounkamhang, "Study on detection of carbaryl pesticides by using surface-enhance raman spectroscopy," *Key Engineering Materials*, vol. 853, pp. 97-101, 2020.
- [2] L. Wipawanee, S. Limwichean, N. Nuntawong, P. Eiamchai, S. Kalasung, O.-U Nimitrakoolchai, and Nongluck Hounkamhang, "Rapid detection of cypermethrin by using surface-enhanced raman scattering technique," *Key Engineering Materials* vol. 853, pp. 102-106, 2020.
- [3] R. Botta, P. Eiamchai, M. Horprathum, S. Limwichean, C. Chananonwathorn, V. Patthanasettakul, R. Maezono, A. Jomphoak, and N. Nuntawong, "3D structured laser engraves decorated with gold nanoparticle SERS chips for paraquat herbicide detection in environments," *Sensors and Actuators B: Chemical*, vol. 304, p. 127327, 2020.
- [4] D. Maddipatla, F. Janabi, B. B. Narakathu, S. Ali, Vi. S. Turkani, B. J. Bazuin, P. D. Fleming, and M. Z. Atashbar, "Development of a novel wrinkle-structure based SERS substrate for drug detection applications," *Sensing and Bio-Sensing Research*, vol. 24, p. 100281, 2019.
- [5] M. Liszewska, B. Bartosewicz, B. Budner, B. Nasiłowska, M. Szala, J. L. Weyher, I. Dziecieliwski, Z. Mierczyk, and B. J. Jankiewicz, "Evaluation of selected SERS substrates for trace detection of explosive materials using portable Raman systems," *Vibrational Spectroscopy*, vol. 100, pp. 79-85, 2019.
- [6] M. Liu, and W. Chen, "Graphene nanosheets-supported Ag nanoparticles for ultrasensitive detection of TNT by surface-enhanced Raman spectroscopy," *Biosensors and Bioelectronics*, vol. 46, pp. 68-73, 2013.
- [7] M. Mou, D. Chen, X. Wang, B. Zhang, T. He, H. Xin, and F. C. Liu, "SERS and UV spectra of meso-tetrakis (4-sulfonatophenyl)-porphine adsorbed on Ag₂O colloids," *Chemical Physics Letters*, vol. 179, no. 3, pp. 237-242, 1991.
- [8] M. Cyrankiewicz, T. Wybranowski, and S. Kruszewski, "Study of SERS efficiency of metallic colloidal systems," *Journal of Physics Conference Series*, vol. 79, no. 1, p. 012013, 2007.
- [9] C. Kavitha, K. Bramhaiah, N. S. John, and B. E. Ramachandran, "Low cost, ultra-thin films of reduced graphene oxide-Ag nanoparticle hybrids as SERS based excellent dye sensors," *Chemical Physics Letters*, vol. 629, pp. 81-86, 2015.
- [10] G. Weng, Y. Yang, J. Zhao, J. Li, J. Zhu, and J. Zhao, "Improving the SERS enhancement and reproducibility of inkjet-printed Au NP paper substrates by second growth of Ag nanoparticles," *Materials Chemistry and Physics*, vol. 253, p. 123416, 2020.
- [11] R. Li, J. Lei, Y. Zhou, and H. Li, "Hybrid 3D SERS substrate for Raman spectroscopy," *Chemical Physics Letters*, vol. 754, p. 137733, 2020.
- [12] A. K. Pal, S. Pagal, K. Prashanth, G. K. Chandra, S. Umapathy, and B. D. Mohan, "Ag/ZnO/Au 3D hybrid structured reusable SERS substrate as highly sensitive platform for DNA detection," *Sensors and Actuators B: Chemical*, vol. 279, pp. 157-169, 2019.
- [13] X. Y. Zhao, G. Wang, and M. Hong, "Hybrid structures of Fe₃O₄ and Ag nanoparticles on Si nanopillar arrays substrate for SERS applications," *Materials Chemistry and Physics*, vol. 214, pp. 377-382, 2018.
- [14] H. Qiu, M. Wang, L. Li, J. Li, Z. Yang, and M. Cao, "Hierarchical MoS₂-microspheres decorated with 3D AuNPs arrays for high-efficiency SERS sensing," *Sensors and Actuators B: Chemical*, vol. 255, pp. 1407-1414, 2018.
- [15] E. Ashok Kumar, N. Riswana Barveen, T. J. Wang, T. Kokulnathan, and Y. H. Chang, "Development of SERS platform based on ZnO multipods decorated with Ag nanospheres for detection of 4-nitrophenol and rhodamine 6G in real samples," *Microchemical Journal*, vol. 170, p. 106660, 2021.
- [16] Q. Wang, C. Zhang, T. Gong, W. Kong, W. Yue, W. Chen, Z. Xie, Y. Su, and L. Li, "Large-scale diamond silver nanoparticle arrays as uniform and sensitive SERS substrates fabricated by surface plasmon lithography technology," *Optics Communications*, vol. 444, pp. 56-62, 2019.
- [17] I. Lettrichova, A. Laurencikova, D. Pudis, J. Novak, M. Gorau, J. Kovac, P. Gaso, and J. Nevrela, "2D periodic structures patterned on 3D surfaces by interference lithography for SERS," *Applied Surface Science*, vol. 461, pp. 171-174, 2018.
- [18] T. Wu, and Y.-W. Lin, "Surface-enhanced Raman scattering active gold nanoparticle/nanohole arrays fabricated through electron beam lithography," *Applied Surface Science*, vol. 435, pp. 1143-1149, 2018.
- [19] N. A. Cinel, S. Cakmakyapan, S. Butun, G. Ertas, E. Ozbay, "E-Beam lithography designed substrates for surface enhanced Raman spectroscopy," *Photonics and Nanostructures - Fundamentals and Applications*, vol. 15, pp. 109-115, 2015.
- [20] R. M. Philip, and D. B. Mohan, "Investigation of chemical inertness of DC magnetron sputtered Bi thin films to the ambient

- conditions for SERS applications,” *Materials Today: Proceedings*, 2021.
- [21] L. Hu, X. Liu, G. Le, J. Li, F. Qu, S. Lu, and L. Qi, “Morphology evolution and SERS activity of the nanoporous Au prepared by dealloying sputtered Au-Ag film,” *Physica B: Condensed Matter*, vol. 558, pp. 49-53, 2019.
- [22] Y. Chen, and Y. Fang, “Surface enhanced Raman scattering (SERS) activity studies of Si, Fe, Ti, Al and Ag films’ prepared by magnetron sputtering,” *Spectrochimica Acta Part A: Molecular and Biomolecular Spectroscopy*, vol. 69, no. 3, pp. 733-737, 2008.
- [23] J. Li, and Y. Fang, “An investigation of the surface enhanced Raman scattering (SERS) from a new substrate of silver-modified silver electrode by magnetron sputtering,” *Spectrochimica Acta Part A: Molecular and Biomolecular Spectroscopy*, vol. 66, no. 4-5, pp. 994-1000, 2007.
- [24] F. Zhang, Y. Zhang, Y. Wang, and X. Zhao, “Composition-dependent LSPR shifts for co-sputtered TiS₂-Ag,” *Optics Communications*, vol. 473, p. 125935, 2020.
- [25] L. Meng, S. Hu, C. Xu, X. Wang, H. Li, and X. Yan, “Surface enhanced Raman effect on CVD growth of WS₂ film,” *Chemical Physics Letters*, vol. 707, pp. 71-74, 2018.
- [26] S.-T. Chen, Y.-C. Chu, C.-Y. Liu, C.-H. Huang, Y. Tzeng, “Surface-enhanced Raman spectroscopy for characterization of nanodiamond seeded substrates and ultrananocrystalline diamond at the early-stage of plasma CVD growth process,” *Diamond and Related Materials*, vol. 24, pp. 161-166, 2012.
- [27] T. Li, Y. Xu, Y. Feng, C. Zhang, C. Yang, Z. Sun, H. Zhang, X. Yuan, T. Ning, and C. Yang, “Self-assembly of the stretchable AuNPs@MoS₂@GF substrate for the SERS application,” *Applied Surface Science*, vol. 423, pp. 1072-1079, 2017.
- [28] T.-L. Guo, J.-G. Li, X. Sun, and Y. Sakka, “Photocatalytic growth of Ag nanocrystals on hydrothermally synthesized multiphasic TiO₂/reduced graphene oxide (rGO) nanocomposites and their SERS performance,” *Applied Surface Science*, vol. 423, pp. 1-12, 2017.
- [29] T. Jiang, B. Wang, L. Zhang, and J. Zhou, “Hydrothermal synthesis of silver nanocubes with tunable edge lengths and their size dependent SERS behaviors,” *Journal of Alloys and Compounds*, vol. 632, pp. 140-146, 2015.
- [30] J. Singh, Rishikesh, S. Kumar, and R. Soni, “Synthesis of 3D-MoS₂ nanoflowers with tunable surface area for the application in photocatalysis and SERS based sensing,” *Journal of Alloys and Compounds*, vol. 849, p. 156502, 2020.
- [31] C. Zanchi, L. Giuliani, A. Lucotti, M. Pistaffa, S. Trusso, F. Neri, M. Tommasini, and P.M. Ossi, “On the performance of laser-synthesized, SERS-based sensors for drug detection,” *Applied Surface Science*, vol. 507, pp. 145109, 2020.
- [32] P. Fu, X. Shi, F. Jiang, and X. Xu, “Superhydrophobic nanostructured copper substrate as sensitive SERS platform prepared by femtosecond laser pulses,” *Applied Surface Science*, vol. 501, pp. 144269, 2020.
- [33] W. Sun, R. Hong, Q. Liu, Z. Li, J. Shi, C. Tao, and D. Zhang, “SERS-active Ag-Al alloy nanoparticles with tunable surface plasmon resonance induced by laser ablation,” *Optical Materials*, vol. 96, pp. 109298, 2019.
- [34] K. K. Maniam and S. Paul, “Corrosion Performance of Electro-deposited Zinc and Zinc-Alloy Coatings in Marine Environment,” *Corrosion and Materials Degradation*, vol. 2, no. 2, pp. 163-189, 2021.
- [35] Z. Wang, J. J. Wang, Y. Lai, Z. Wei, and J. Li, “Rapid detection of estrogen compounds using surface-enhanced Raman spectroscopy with a Zn/Au-Ag/Ag sandwich-structured substrate,” *Optical Materials*, vol. 112, p. 110759, 2021.
- [36] K. Lv, H. Si, J. Liu, T. Zhu, Y. Xia, S. Chen, Y. Zhao, and C. Yang, “Plasmonic filters based on MoS₂@Au/Ag hybrids: Controllable separation, preconcentration, and sensitive SERS detection,” *Journal of Alloys and Compounds*, vol. 846, p. 156438, 2020.
- [37] S. Kundu, W. Dai, Y. Chen, L. Ma, Y. Yue, A. M. Sinyukov, and H. Liang, “Shape-selective catalysis and surface enhanced Raman scattering studies using Ag nanocubes nanospheres and aggregated anisotropic nanostructures,” *Journal of Colloid and Interface Science*, vol. 498, pp. 248-262, 2017.
- [38] L. Wu, W. Zhang, C. Liu, M.F. Foda, and Y. Zhu, “Strawberry-like SiO₂/Ag nanocomposites immersed filter paper as SERS substrate for acrylamide detection,” *Food Chemistry*, vol. 328, p. 127106, 2020.
- [39] Q. Li, S. Gong, H. Zhang, F. Huang, L. Zhang, and S. Li, 2019. “Tailored necklace-like Ag@ZIF-8 core/shell heterostructure nanowires for high-performance plasmonic SERS detection,” *Chemical Engineering Journal*, vol. 371, pp. 26-33, 2019.